LAWRENCE
LIVERMORE
NATIONAL
LABORATORY

LLNL-PROC-676417

Using the XFEL to drive the gain of inner-shell X-ray lasers using photoionization and photoexcitation processes

J. Nilsen

August 19, 2015

X-ray Lasers and Coherent X-ray Sources: Development and Applications XI
San Diego, CA, United States
August 12, 2015 through August 13, 2015

Disclaimer

Using the XFEL to drive the gain of inner-shell X-ray lasers using photoionization and photoexcitation processes

Joseph Nilsen

Lawrence Livermore National Laboratory, Livermore, CA 94551

ABSTRACT

Four years ago an inner-shell X-ray laser was demonstrated at 849 eV in singly ionized neon gas using the LCLS X-FEL at 960 eV to photo-ionize the 1s electron in neutral neon followed by lasing on the 2p – 1s transition in singly-ionized neon. It took many decades to demonstrate this scheme because it required a very strong X-ray source that could photo-ionize the 1s (K shell) electrons in neon on a time scale comparable to the intrinsic auger lifetime in the neon, which is typically 2 fsec. In this work we model the neon inner shell X-ray laser under similar conditions to those used at LCLS and investigate how we can improve the efficiency of the neon laser and reduce the drive requirements by tuning the X-FEL to the 1s-3p transition in neutral neon in order to create gain on the 2p-1s line in neutral neon. We also explore using the XFEL to drive gain on 3-2 transitions in singly-ionized Ar and Cu plasmas.

Keywords: X-FEL; inner-shell X-ray laser

1. INTRODUCTION

In the 1960's while working at Bell Laboratories where the laser was invented, Duguay and Rentzepis proposed using photo-ionization to create an X-ray laser on the inner shell K-α line in sodium vapour [1]. A decade later in the 1970's Ray Elton [2] discussed the challenges of making quasi steady state inner-shell K-α lasers in Si, Ca, and Cu. In 2011 the dream of demonstrating an inner-shell X-ray laser was realized at the SLAC Linac Coherent Light Source (LCLS) when the X-ray free electron laser (XFEL) at 960 eV was used to photo-ionize the K-shell of neutral neon gas and create lasing at 849 eV in singly ionized neon gas [3].

In this paper we look at the advantages and challenges of using the XFEL to resonantly photo-pump the 1s-3p line in neutral neon as a mechanism for creating gain on the K-α line in Ne and compare this with the photo-ionization pumping that has already been demonstrated. We show that with the use of a sufficiently short XFEL pulse (1-fsec) the resonant photo-excitation could reduce the XFEL flux requirements by several orders of magnitude.

We then look at how the inner-shell X-ray laser can be extended to lasing on L-shell transitions in Ar and Cu.

2. MODELLING THE INNER-SHELL NE LASER

The pumping mechanism used in the LCLS experiments that demonstrated lasing on the inner-shell neon laser is shown in Fig. 1. The XFEL beam is tuned above the K-edge of neutral Ne I in order to photo-ionize the 1s electron. This creates an excited state of singly ionized Ne II that has a missing 1s electron. This excited state then lases to the ground state of Ne II by emitting an X-ray on the 2p – 1s transition at 848.6 eV. The experiment starts with neon gas that is in the Ne I ground state. The lower laser state is initially unoccupied. The natural lifetime of the laser transition is 135 fsec.

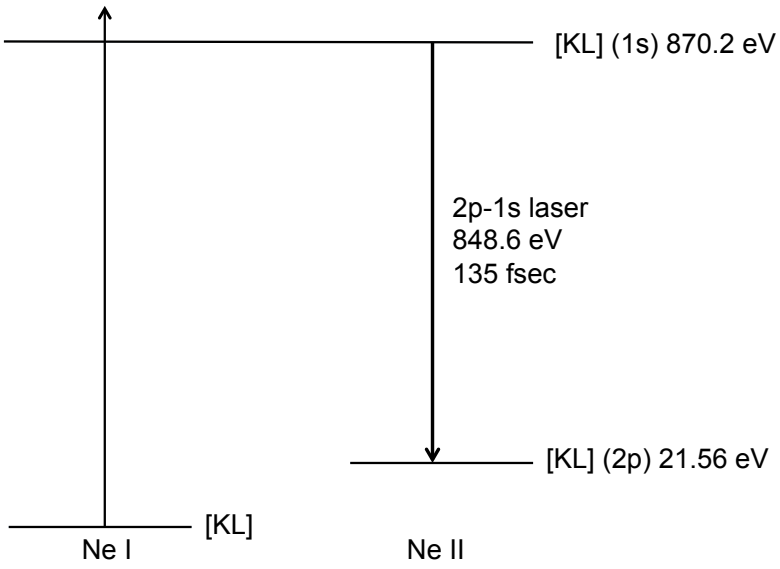

Fig. 1. Energy level diagram for the photo-ionization driven inner-shell neon X-ray laser.

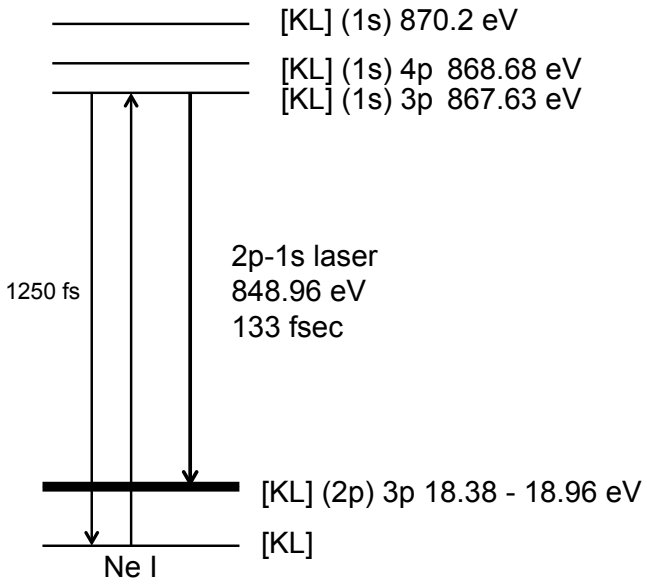

Fig. 2. Energy level diagram for the photo-excitation driven inner-shell neon X-ray laser.

The notation [KL] signifies closed K shell, $1s^2$, and L shell, $2s^22p^6$, configurations while the (2p) stands for a 2p hole in the L shell. The challenge with this scheme is that the Auger lifetime of the upper laser state is 2.3 fsec so pumping this scheme requires a very short pulse duration in the fsec regime. Figure 2 shows the resonant photo-pumping mechanism for driving the inner-shell neon laser. In this case, the XFEL is tuned to the 1s – 3p transition in Ne I at 867.63 eV creating a large population in the $1s2s^22p^63p$ level. This level can then lase to the lower $1s^22s^22p^53p$ level state by emitting X-rays on the 2p – 1s transition centered at 848.96 eV. Because of the splitting in the lower level state there are 5 X-ray lines emitted that are spread over the energy range from 848.67 to 849.25 eV. We calculate the total gain by summing the gain of the 5 lines. The upper laser level has a similar Auger lifetime of 2.3 fsec that implies a line-width of 0.3 eV on the lasing transition. The photo-excitation scheme also requires a short pulse drive because of the very short Auger lifetime. The difference between this scheme and the photo-ionization scheme is that lasing in now in neutral Ne I instead of Ne II. The lasing energies differ by about 0.4 eV. The potential advantage of this scheme is that the photo-excitation cross-section is about 18 Mbarns compared to 0.3 Mbarns for the photo-ionization scheme. In this paper we show how we can take advantage of this much larger excitation rate to reduce the drive requirements on the XFEL source.

We created a simple atomic model of the levels shown in Figs. 1 and 2. We used the kinetics code Cretin [4] to model the kinetics and gain of the system under various conditions assuming a Ne gas with an ion density of 2 x $10^{19}/cm^3$. For the baseline XFEL beam we assume the XFEL beam has 10^{12} photons in a 0.9 eV line-width focused to a 1-μm diameter. For the pulse duration we compare a Gaussian shape with 100-fsec full-width half-maximum (FWHM) to a 1-fsec FWHM. The XFEL was designed to have a bandwidth of 0.1% as we are assuming even though the current bandwidth is larger by a factor of 5-10. The bandwidth has minimal impact on the photo-ionization mechanism but the strength of the photo-excitation mechanism is inversely proportional to the bandwidth. One challenge with the photo-excitation scheme is understanding the validity of the kinetics model and how to include the photo-excitation rate in the line-width calculation of the gain. Currently the stimulated rate is included in the kinetics but not in the line-width which means there are no Stark sidebands or broadening. The XFEL energy is set at 875 eV for modelling the photo-ionization scheme and 867.6 eV for modelling the photo-excitation scheme.

Starting with a 100-fsec duration XFEL pulse, Fig. 3 shows the predicted gain versus time for both schemes. Time = 0 is defined as the peak of the XFEL pulse. To understand the sensitivity to the XFEL flux a series of calculations were done using a multiplier between 1.0 (nominal) and 0.001 on the nominal XFEL flux described above. For the photo-ionization scheme using the nominal intensity with multiplier of 1.0 we predict peak gain of 44 cm^{-1} at a time 81 fsec before the peak of the XFEL drive. In contrast the peak gain of 62 cm^{-1} for the photo-excitation scheme occurs 128 fsec before the peak of the XFEL. The big difference between the behavior of the two schemes is that the gain of the photo-excitation scheme falls much slower as the XFEL flux is reduced. With a multiplier of 0.001, which corresponds to 10^9 photons in the beam, the peak gain is still 12 cm^{-1} at t = -12 fsec as compared with 0.7 cm^{-1} for the photo-ionization scheme. For both schemes, the peak gain starts before the peak of the XFEL pulse and moves closer to t=0 as the flux is reduced. To optimize the XFEL drive one wants the peak gain to occur at the peak of the XFEL drive pulse, otherwise some of the XFEL drive is not being used.

Now consider a 1-fsec duration XFEL driving the Ne gas a shown in Fig. 4. For the nominal XFEL flux the peak gains are 910 cm^{-1} at 0.5 fsec before the peak of the XFEL drive for the photo-ionization case and 703 cm^{-1} at 1.1 fsec before the peak of the XFEL drive for photo-excitation. As the flux intensity is reduced the gain for the photo-ionization drops quickly but one notices that the peak gain for the photo-excitation scheme drops from 703 cm^{-1} to 639 cm^{-1} as the XFEL drive flux is reduced by a factor of 100. Also the peak of the gain moves to a time of -0.2 fsec, indicating near optimum drive conditions. As the XFEL flux drops further the gain drops more quickly and occurs after the peak of the XFEL flux indicating the flux is below ideal drive conditions. This figure shows that the photo-excitation mechanism offers the potential to reduce the XFEL drive by two orders of magnitude as compared with the photo-ionization mechanism. This advantage could enable smaller facilities to drive inner shell X-ray lasers or allow facilities such as LCLS to drive even higher energy X-ray lasers with the current XFEL fluxes.

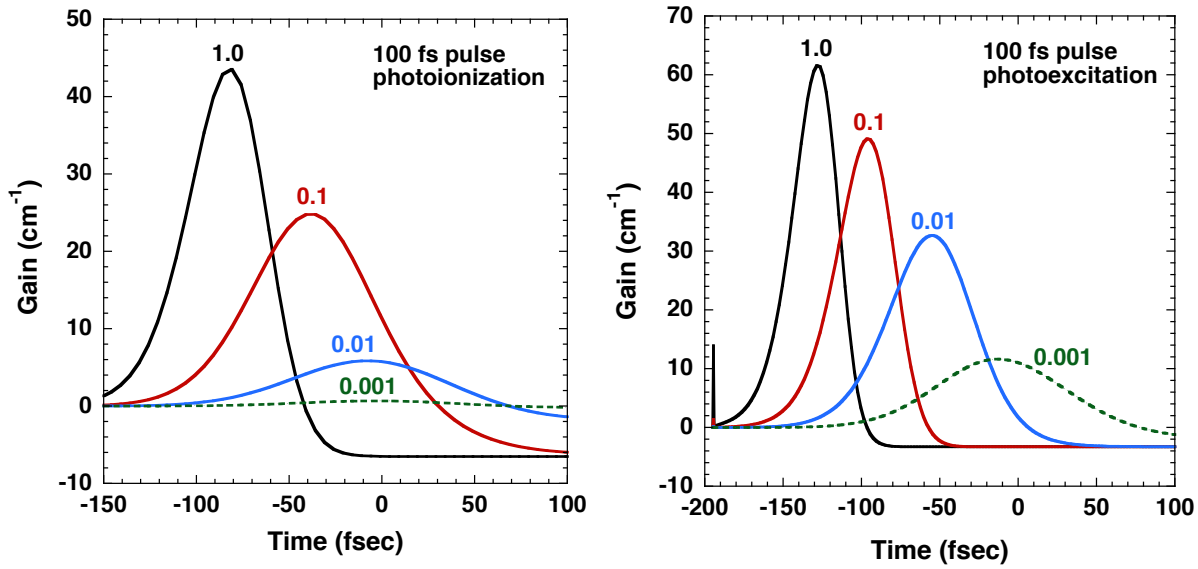

Fig. 3. Gain versus time for the neon X-ray laser driven by a 100-fs duration XFEL comparing the photo-ionization and photo-excitation mechanisms. The XFEL intensity is varied by using multipliers of 1.0 (nominal), 0.1, 0.01, and 0.001.

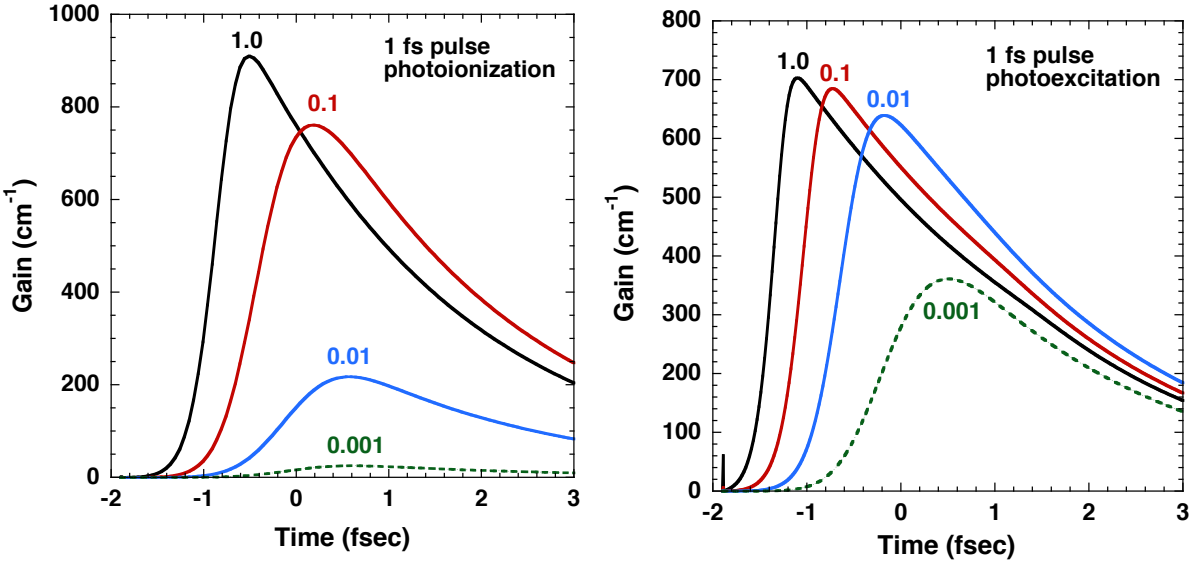

Fig. 4. Gain versus time for the neon X-ray laser driven by a 1-fs duration XFEL comparing the photo-ionization and photo-excitation mechanisms. The XFEL intensity is varied by using multipliers of 1.0 (nominal), 0.1, 0.01, and 0.001.

3. MODELLING INNER-SHELL AR AND CU LASERS

With the success of the K-shell neon X-ray laser it should be possible to demonstrate inner-shell X-ray lasers in other principal shells such as the L and M shells. A promising candidate to consider is neutral argon gas. Figure 5 shows the energy level diagram for using an XFEL above the L-shell edge of neutral Ar I to create a L-shell hole in singly ionized Ar II. If an XFEL was tuned between the two L-edges at 248 and 326 eV one could create a 2p hole that would result in lasing on the 3s-2p transition at 232.7 eV. If the XFEL drive was tuned above the L-edge at 326.3 eV then one would have holes in both the 2s and 2p shells that would result in lasing on the 3p-2s transition at 310.6 eV as well as the 3s-2p transition. It would be possible to tune the XFEL from low to high energy and watch the 3s-2p lasing turn on followed by lasing on both lines.

Figure 6 shows the energy level diagram for using an XFEL above the L-shell edges of neutral Cu I to create a L-shell (2p) hole in singly ionized Cu II and create lasing on the strong 3d-2p lines at 928 and 948 eV. As an alternative, photo-excitation of the 2p-4d transition in Cu I would also create lasing on the 3d-2p line in Cu I analogous to the Ne case discussed in the previous section. One advantage of Cu over Ar is that the M-shell is full and therefore one can obtain lasing on the 3d-2p lines that have larger emission rates than the 3s-2p and 3p-2s transitions used in Ar.

To model this we created a simple atomic model of Cu with the Cu I ground state, 4 levels in Cu II as shown in Fig. 6, and 2 levels in Cu III. We assumed the Auger lifetime for the LMM transitions was 2.3 fs, similar to the KLL rates in Ne. In the modeling the absorption oscillator strength for the 948 eV line is half of the 928 eV line and the calculated gain tends to be about half of the 928 eV line. As a result we only plot the gain for the 928 eV line in Fig. 7.

To model the gain we assume the nominal XFEL beam has 10^{12} photons at a photon energy of 1 keV in a 1.0 eV line-width focused to a 1-μm diameter. For the pulse duration we compare a Gaussian shape with 100-fsec full-width half-maximum (FWHM) to a 10-fsec FWHM. The Cu is assumed to be a gas at an ion density of $2 \times 10^{19}/cm^3$. Figure 7 plots the gain of the 928 eV line versus time for the cases where the 100-fs XFEL pulse is reduced in intensity by multipliers varying from 1 to 0.01. Time = 0 is defined as the peak of the XFEL pulse. Using the nominal intensity with multiplier of 1.0 we predict peak gain of 31 cm^{-1} at a time 101 fsec before the peak of the XFEL drive. As the intensity is reduced by a factor of 10 the peak gain drops to 22 cm^{-1} while reducing the intensity by 100 gives a peak gain of 8.9 cm^{-1} at 21 fs before the peak of the XFEL drive.

Keeping the same 10^{12} photons we reduced the pulse duration to 10 fsec and looked at the sensitivity of the gain for the 928 eV line versus time as a function of XFEL drive intensity. The peak gain for the nominal case is now 136 cm^{-1} but a tenfold reduction in intensity only drops it to 126 cm^{-1} and moves the peak closer to zero time as shown in Fig. 7. A further tenfold reduction (multiplier = 0.01) still yields a peak gain of 84 cm^{-1} that now coincides with the time of peak XFEL drive. This suggests we could use a much smaller XFEL system or drive gain in a much larger volume if we had the shorter 10 fs pulse available. At the same time we predict peak gain of 43 cm^{-1} on the 948 eV line. Future work will look at even shorter pulse durations.

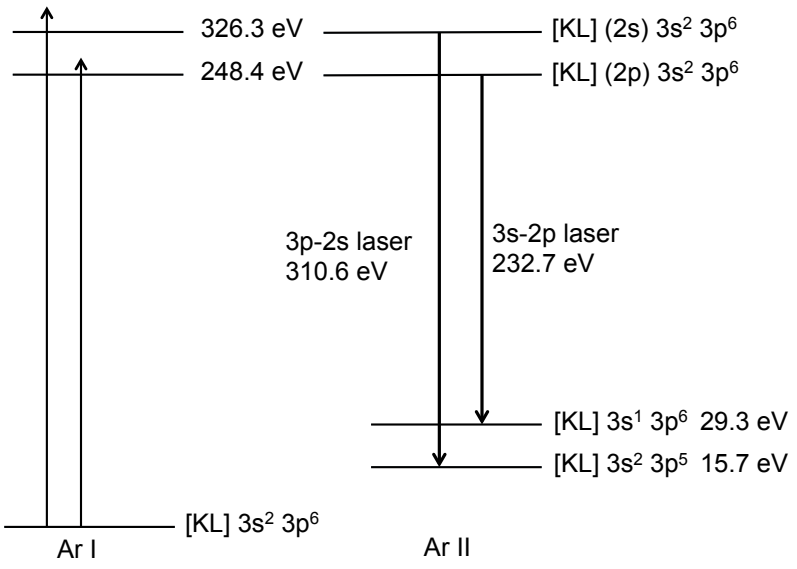

Fig. 5. Energy level diagram for the photo-ionization driven inner-shell argon X-ray laser.

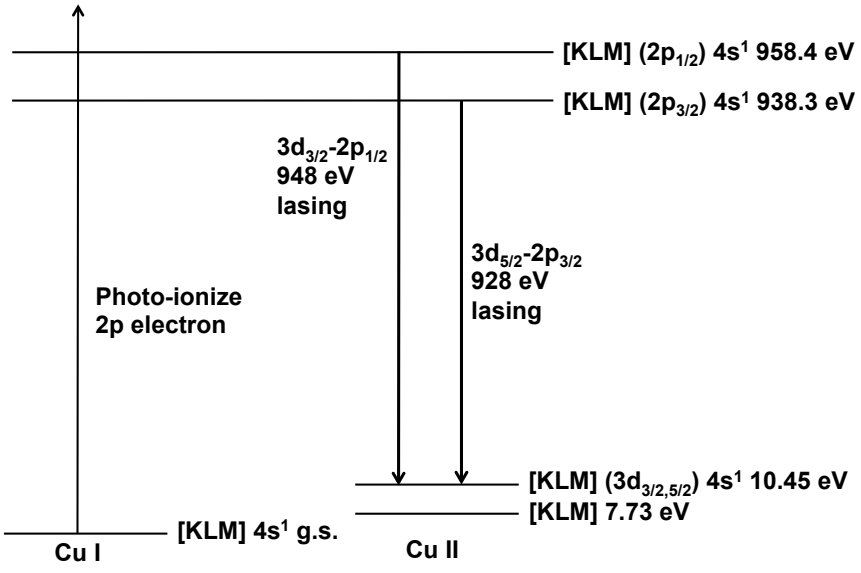

Fig. 6. Energy level diagram for the photo-ionization driven inner-shell copper X-ray laser.

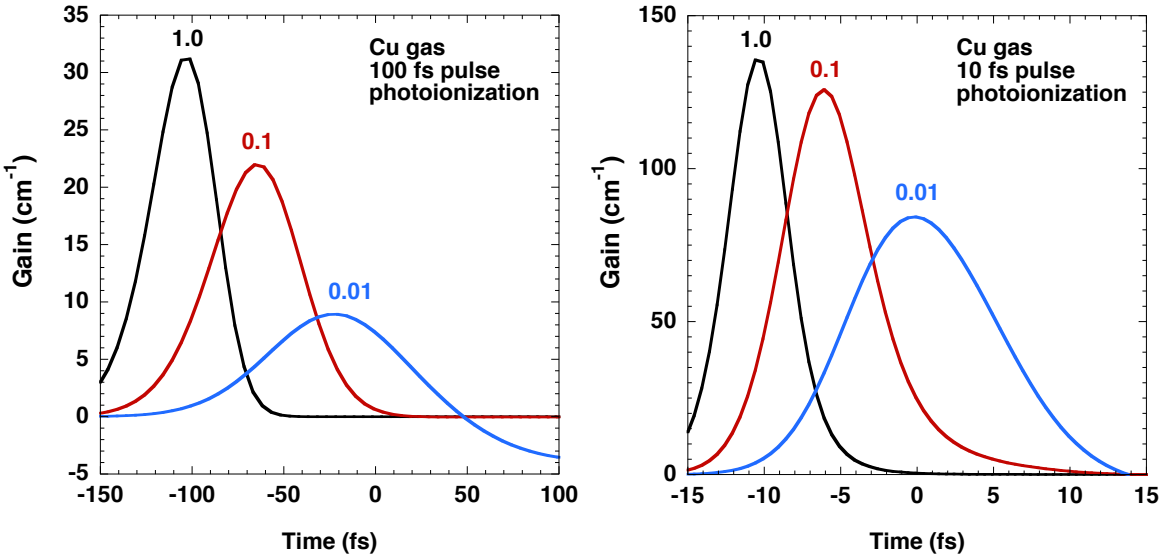

Fig. 7. Gain versus time for the copper X-ray laser driven by the photo-ionization mechanisms and comparing 10-fs and 100-fs duration XFEL drives. The XFEL intensity is varied by using multipliers of 1.0 (nominal). 0.1, 0.01, and 0.001.

4. CONCLUSIONS

In this paper we model the neon inner shell X-ray laser under similar conditions to those used in the experiments at LCLS that demonstrated the Ne II lasing at 849 eV. We discuss how we can improve the efficiency of the neon laser and reduce the drive requirements by tuning the XFEL to the 1s-3p transition in neutral neon in order to create gain on the 2p-1s line in neutral neon. We present the sensitivity to the drive intensity, pulse duration, and line-width of the XFEL to better understand how to optimize this inner shell laser by understanding the trade-offs between using photo-ionization versus photo-excitation to drive gain in these systems. We show that with the use of a sufficiently short XFEL pulse (1-fsec) the resonant photo-excitation could reduce the XFEL flux requirements by several orders of magnitude. We also discuss how photo-ionization of L-shell electrons can be used to create lasing on n=3-2 transitions in materials such as Ar at 232 and 310 eV and Cu at 928 and 948 eV.

ACKNOWLEDGEMENTS

This work was performed under the auspices of the U.S. Department of Energy by Lawrence Livermore National Laboratory under Contract DE-AC52-07NA27344.

REFERENCES

[1] Duguay, M. A. and Rentzepis, P. M., "Some approaches to vacuum UV and Xray lasers,"Appl. Phys. Lett. **10**, 350–352 (1967).

[2] Elton, R. C., "Quasi-stationary population inversion on Kα transitions," Appl. Opt. **14**, 2243- 2249 (1975).

[3] Rohringer, N., Ryan, D., London, R. A., Purvis, M., Albert, F., Dunn, J., Bozek, J. D., Bostedt, C., Graf, A., Hill, R., Hau-Riege, S. P., and Rocca, J. J., "Atomic inner-shell X-ray laser at 1.46 nanometres pumped by an X-ray free-electron laser," Nature 481, 488–491 (2012).

[4] Scott, H. A., "Cretin – a radiative transfer capability for laboratory plasmas," JQSRT **71**, 689–701 (2001).